Phytopathology Research

RESEARCH

Open Access

The *Puccinia triticina* effector Pt3372 suppresses wheat innate immunity by targeting wheat TaERP3 in TcLr2a and TcLr18

Xiaolei Wen[1,2], Hao Li[1], Jianyuan Li[1,3], Johannes Mapuranga[1], Na Zhang[1], Lulu Song[1], Jiaying Chang[1], Ruolin Li[1], Yue Zhang[1,4], Daqun Liu[1] and Wenxiang Yang[1*]

Abstract

Puccinia triticina (*Pt*) is an obligate parasitic fungus that absorbs nutrients through haustoria during infection and secretes a repertoire of effector proteins into the host cells to regulate the immune response of the host. Here, we identify an effector protein Pt3372 from the transcriptome data of interaction between the *Pt* race JHKT and the susceptible wheat cultivar Thatcher. Pt3372 was highly induced at the early stages in TcLr2a and TcLr18 infected by JHKT. The effector inhibited cell death induced by BAX (Bcl2-associated X) and INF1 (*Phytophthora infestans* INF1) in *Nicotiana benthamiana*, as well as cell death induced by *Pseudomonas syringae* pv. tomato DC3000 in wheat. Pt3372 was proved to be localized in the cell membrane and nucleus of *N. benthamiana*. When transiently expressed in TcLr2a and TcLr18 through the bacterial type III secretion system, Pt3372 inhibited callose deposition and reactive oxygen species accumulation and suppressed the expression of wheat pathogenesis-related genes *PR1* and *PR2*. Silencing *Pt3372* by host-induced gene silencing reduced the *Pt* race JHKT virulence on TcLr2a and TcLr18. While it was enhanced by the overexpression of Pt3372 in transgenic wheat, which had a down-regulated expression of *TaPR2* and glutathione reductase *TaGR*. Moreover, Pt3372 targets the elicitor-responsive protein TaERP3. Altogether, our results demonstrate that the effector Pt3372 suppresses the expression of *TaPR1* and *TaPR2* and the innate immunity by targeting the TaERP3.

Keywords *Puccinia triticina*, Effector protein, Resistance, Host–pathogen interaction, Pathogenesis

Background

Naturally, many plants exhibit a remarkable level of resistance towards a wide array of pathogens. However, certain pathogenic microbes can cause serious diseases. Plant defense mechanisms include constitutive preformed and induced defense responses, which provide multiple layers of protection against pathogen invasion (Anderson et al. 2010). The detection of conserved pathogen-associated molecular patterns (PAMPs) by membrane-localized pattern recognition receptors (PRRs) triggers the first layer of host inducible immunity known as PAMP-triggered immunity (PTI) (Boller and Felix 2009). Plants transmit downstream immune signals through cytoplasmic receptor kinase BIK1 (*Botrytis-induced kinase* 1),

*Correspondence:
Wenxiang Yang
wenxiangyang2003@163.com
[1] College of Plant Protection, Hebei Agricultural University, Technological Innovation Center for Biological Control of Plant Diseases and Insect Pests of Hebei Province / National Engineering Research Center for Agriculture in Northern Mountainous Areas, Baoding 071000, China
[2] College of Agronomy and Biotechnology, Hebei Normal University of Science and Technology / Hebei Key Laboratory of Crop Stress Biology, Qinhuangdao 066000, China
[3] College of Biological Sciences and Engineering, Xingtai University, Xingtai 054000, China
[4] Institute of Dry Land Farming, Hebei Academy of Agriculture and Forestry Sciences, Shijiazhuang 050000, China

© The Author(s) 2025. **Open Access** This article is licensed under a Creative Commons Attribution 4.0 International License, which permits use, sharing, adaptation, distribution and reproduction in any medium or format, as long as you give appropriate credit to the original author(s) and the source, provide a link to the Creative Commons licence, and indicate if changes were made. The images or other third party material in this article are included in the article's Creative Commons licence, unless indicated otherwise in a credit line to the material. If material is not included in the article's Creative Commons licence and your intended use is not permitted by statutory regulation or exceeds the permitted use, you will need to obtain permission directly from the copyright holder. To view a copy of this licence, visit http://creativecommons.org/licenses/by/4.0/.

MAPK cascade, and CDPKs (Calcium-dependent protein kinases), which induce the bursting of reactive oxygen species, callose deposition, stomatal closure, and expression of defense-related genes, thereby inhibiting pathogen growth and proliferation (Kunze et al. 2004; Miya et al. 2007; Shimizu et al. 2010; Kadota et al. 2015; Gupta et al. 2020). In order to overcome the host PTI, pathogens secrete a repertoire of effector proteins into plant cells that will suppress the host immune responses. However, plants evolved intracellular nucleotide-binding leucine-rich repeat (NLR) immune receptors that specifically recognize effector proteins and trigger a second layer of defense response known as effector-triggered immunity (ETI), which is associated with hypersensitive response (HR) in host cells (Jones and Dangl 2006).

Wheat leaf rust caused by *Puccinia triticina* (*Pt*) is an important disease on wheat around the world, which seriously threatens the food security of wheat. In severe cases, it can cause a loss of 15–40%, and in areas with a suitable environment, it can cause a loss of 75% (Kolmer 2005; Huerta-Espino et al. 2011; Savary et al. 2019; Abebe 2021). Long-term monoculture of resistant wheat cultivars and the emergence of new physiological races are the main reasons for the loss of resistance in wheat cultivars. The physiological race 4 of *Pt* was first discovered in the 1970s, and it became the dominant race in 1986, resulting in a large area of leaf rust (Zhang et al. 2019; Zhang et al. 2020a, b). In recent years, the dominant races of *Pt* in China have gradually changed, with physiological races such as THTT and PHTT being dominant every year. Leaf rust has gradually overcome the main wheat leaf rust resistance genes such as *Lr1*, *Lr10*, *Lr26*, *Lr2a,* and *Lr18* in China (Zhang et al. 2019; Zhang et al. 2020a, b). It has exerted great pressure on wheat leaf rust resistance breeding, rust prevention, and control through the deployment of disease-resistant cultivars in China. Therefore, it is important to understand the mechanisms underlying the interaction between *Pt* and how the pathogen overcomes wheat disease resistance genes. This will aid in developing new targets for wheat leaf rust prevention and control, unraveling new ways of durable resistance to wheat leaf rust, and solving the resistance breeding bottleneck of limited durable leaf rust disease resistance breeding resources.

The effector protein is a favorable 'weapon' for pathogen infection, which interferes with the host's immune system in a variety of ways. For example, the LysM effector protein Ecp6 of *Cladosporium fulvum* can bind to chitin oligosaccharides to prevent the recognition of chitin polymers by host surface receptors, thereby inhibiting the activation of host chitin-triggered immunity (de Jonge et al. 2010). The *Phytophthora infestans* RXLR effector SF15 suppresses host immunity by interacting with CaM, which interferes with immune signaling components (Zheng et al. 2018). *Puccinia striiformis* f. sp. *tritici* (*Pst*) glycine-serine-rich effector protein PstGSRE4 without m9-like motif modulates wheat immunity by inhibiting the enzyme activity of TaCZSOD2, a wheat copper-zinc superoxide dismutase (Liu et al. 2022). Pst_12806 enhances pathogen virulence by targeting the Rieske domain of TaISP to reduce the rate of photosynthesis and inhibits ROS accumulation (Xu et al. 2019). PNPi inhibits multiple wheat defense responses by interacting with the pathogenicity-related protein TaPR1a in the apoplast (Bi et al. 2020). Pst18363 promotes pathogen infection by targeting and stabilizing TaNUDX23, which inhibits the accumulation of ROS (Yang et al. 2020). The effector protein PstCFEM1, containing an extracellular membrane domain, inhibits the wheat defense response by suppressing ROS accumulation (Bai et al. 2022). Pst27791 inhibits ROS accumulation and salicylic acid-dependent defense response by targeting wheat Raf-like kinase TaRaf46 (Wan et al. 2022). Furthermore, *Pst* effectors PSTha5a23 (Cheng et al. 2017), Pst_8713 (Zhao et al. 2018), PSEC2, PSEC17, and PSEC45 (Su et al. 2021) enhance pathogen virulence by suppressing host PTI response.

Pt effectors suppress multiple wheat defense responses. Nevertheless, the research on *Pt* effector proteins is still lagging behind that of other rust fungi. There are few reports on the molecular mechanisms underlying the regulation of wheat immunity by *Pt* effector proteins. For instance, two secreted proteins were found to induce the transient expression of *β*-glucuronidase in wheat near-isogenic lines containing *Lr9*, *Lr24*, and *Lr26* (Segovia et al. 2016). Pt_21 inhibits leaf rust resistance in wheat by interacting with TaTLP1 (Wang et al. 2023). Pt13024 (Qi et al. 2023), AvrLr15 (Cui et al. 2024), and Pt1641 (Chang et al. 2024a) are avirulent effectors to TcLr30, TcLr15 and TcLr1, respectively. Pt9226 was reported to be virulent to TcLr15 (Wang et al. 2024). Pt9029 suppresses wheat resistance and promotes the pathogenicity of *Pt* by targeting TaRCA (Chang et al. 2024b). Furthermore, Pt1234 modulates wheat immunity by interacting with the TaNAC069 transcription factor through its C subdomain (Geng et al. 2024). Altogether, these studies demonstrate that *Pt* effectors can manipulate the activity of their targets in wheat or inhibit the wheat immune defense responses by acting as enzymes or other roles. However, the mechanisms by which *Pt* effector proteins interact with their host targets are still unclear.

Herein, the effector Pt3372 was obtained from the RNA-seq library constructed by Zhang et al (2020a, b) (https://dataview.ncbi.nlm.nih.gov/object/PRJNA609405?reviewer=j2png1bo7u3jlpp6h3amhk0jfm) and was highly expressed in the early stage of wheat leaf rust infection. When tested in 11 wheat leaf rust-resistant

near-isogenic lines, Pt3372 could inhibit the accumulation of callose in TcLr2a and TcLr18. Therefore, to better understand the molecular mechanisms underlying the role of Pt3372 during *Pt* infection, it was successfully cloned and functionally characterized. qRT-PCR analysis found that *Pt3372* was highly expressed at 6 h after inoculation in TcLr18 and TcLr2a. Subcellular localization and inhibition of cell death induced by BAX and INF1 of Pt3372 were analyzed using the transient expression system in *Nicotiana benthamiana*. A bacterial type III secretion system (T3SS) was used to analyze the ability of Pt3372 to inhibit callose deposition, ROS accumulation, and the expression of pathogenesis-related (*PR*) genes in wheat near-isogenic lines TcLr2a and TcLr18. Silencing *Pt3372* by host-induced gene silencing reduced the *Pt* race JHKT virulence on TcLr2a and TcLr18, and overexpression of *Pt3372* in transgenic wheat enhanced *Pt* virulence and down regulated the expression of *TaPR2* and glutathione reductase *TaGR*. All those demonstrated that the function of Pt3372 during infection was virulent to TcLr2a and TcLr18. Yeast two-hybrid, bimolecular fluorescence complementation (BiFC), and co-immunoprecipitation (Co-IP) assays were employed and showed that Pt3372 targeted TaERP3. We concluded that Pt3372 suppresses the immunity of TcLr2a or TcLr18 by targeting TaERP3. This work unravels new insights into the molecular mechanisms of *Pt* effectors in regulating wheat immunity.

Results

Pt3372 is a secreted protein and is highly expressed during the early stages of *Pt* (JHKT) infection

The gDNA of *Pt3372* is 602 bp, with two introns and three exons. The CDS is 420 bp and encodes a small protein with 139 amino acids (aa) (Fig. 1a), and the first 24 aa (Fig. 1a) of N-terminal presented as a predicted signal peptide and had a hydrophobic structure, but no transmembrane domain. Pt3372 was highly expressed in the early stage of JHKT infection in TcLr2a and TcLr18, and compared with non-germinated urediospores, the expression level reached its peak at 6 hpi (Fig. 1b, c, respectively). These results indicated that Pt3372 is a secreted effector protein. National Center for Biotechnology Information (NCBI) blast showed that Pt3372 was a hypothetical protein and had 100% homology with the putative protein PTTG_25108 of BBBD in *Pt*. The SOPMA analysis showed that there were 42.45% α-helix, 11.51% β-turn, 16.55% extended chain, and 29.5% random coil in the secondary structure of Pt3372. In order to detect whether Pt3372 is species-specific among different *Pt* isolates, we compared the amino acid sequences of 9 *Pt* races with different virulence. The results showed

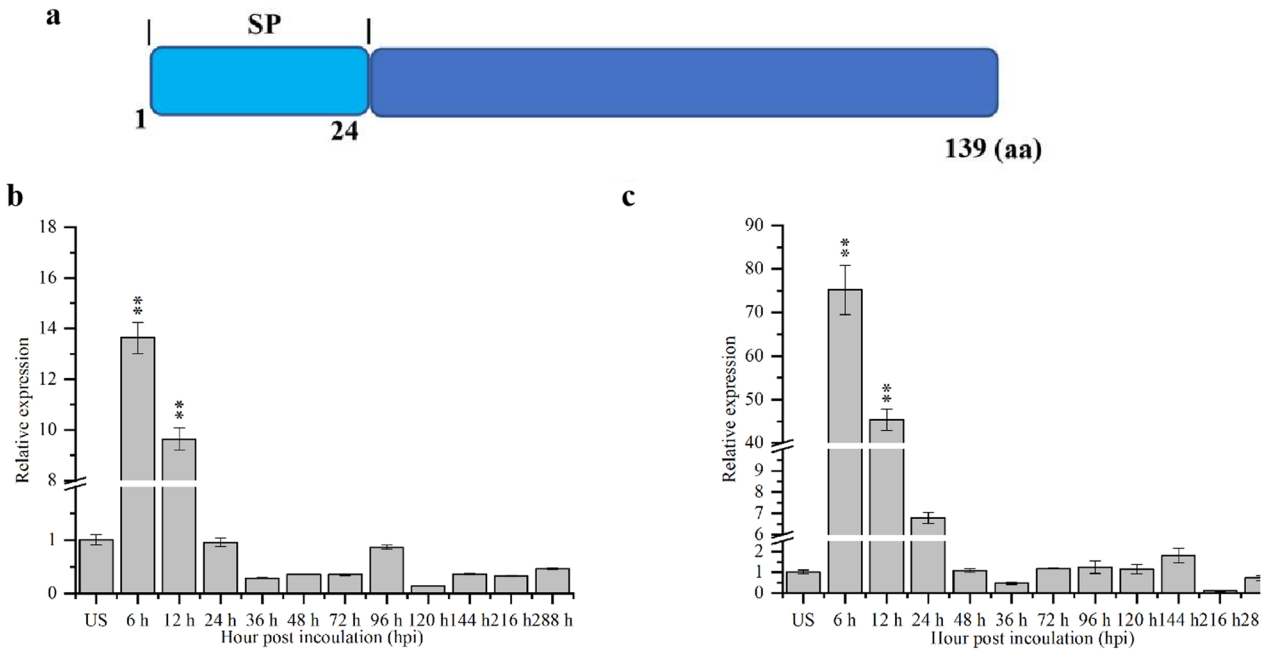

Fig. 1 The structural and expression analysis of Pt3372 in wheat infected by *Puccinia triticina*. **a** The structure of Pt3372,.SP: the signal peptide. **b**, **c** The expression patterns of *Pt3372* in wheat near isogenic lines; TcLr2a and TcLr18 infected by physiological race JHKT of wheat leaf rust. The relative gene expression was calculated by the comparative Ct method with *Pt* endogenous gene *PtActin* as an internal standard and was relative to that of US. US: Urediniospores; Three technical and biological replicates for each treatment were analyzed. The signifcant diference was calculated by t-test, Asterisks indicate significant differences (** $p < 0.01$)

that Pt3372 had neither amino acid in/del no SNPs in different *Pt* physiological races, indicating that Pt3372 is a conservative effector among *Pt* races.

The signal peptide of Pt3372 has a secretory function

The yeast signal peptide trap screen (Jacobs et al. 1997) and 2,3,5-triphenyltetrazolium chloride (TTC) assays were used to identify whether the Pt3372 signal peptide has a secretory function. The results showed that the yeast transformants of the recombinant vector pSUC2-SP3372, negative control pSUC2-Mg87, and positive control pSUC2-Avr1b had tryptophan operons. Different concentrations of yeast could grow on SD/-Trp medium, but wild-type YTK12 could not grow on the medium due to the lack of operons. In YPRAA medium, pSUC2-SP3372 and positive control pSUC2-Avr1b could grow in three different concentrations of yeast solution. On the contrary, negative control pSUC2-Mg87 and wild-type strain YTK12 could not grow normally on YPRAA medium due to a lack of signal peptide sequence. Compared with pSUC2-SP3372 and positive control pSUC2-Avr1b, the growth of pSUC2-Mg87 and YTK12 was significantly inhibited (Fig. 2a). YTK12, which carries pSUC2-Pt3372 and pSUC2-Avr1b, secretes sucrase, which could hydrolyze sucrose into monosaccharides. The monosaccharides reacted with TTC to produce water-insoluble triphenylformazan (TPF), which appeared red. YTK12, pSUC2-Mg87, and pSUC2-Pt3372$^{\Delta SP}$ yeast strains could not secrete sucrase to cause a reaction with TTC (Fig. 2b). These results demonstrate that the putative N-terminal signal peptide of Pt3372 has a secretory function.

Pt3372 is localized in the nucleus and cell membrane

In order to clarify the subcellular localization of Pt3372, we transformed the Pt3372:GFP fusion protein into *Agrobacterium* GV3101 and infiltrated it into *N. benthamiana* leaves. After 48–72 h of dark growth, the fluorescence expression of the leaves was observed under a fluorescence microscope. It was found that Pt3372-GFP and GFP were successfully expressed in tobacco leaves, and the control GFP showed fluorescence in the whole cell. The fusion protein Pt3372-GFP emitted fluorescence signals in the nucleus and cell membrane, indicating that it

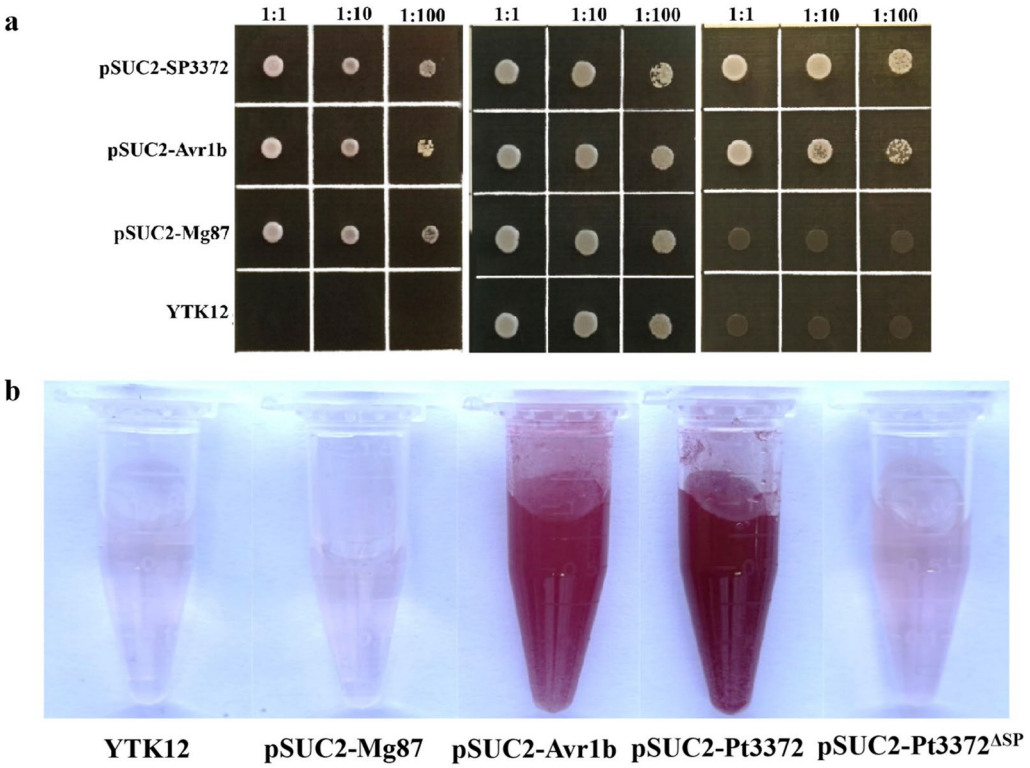

Fig. 2 Pt3372 signal peptide has a secretory function. Functional validation of the putative N-terminal signal peptide of Pt3372 was carried out using the yeast invertase secretion assay and with 2,3,5-triphenyltetrazoliu chloride (TTC). **a** The recombinant vector pSUC2-SP3372 carrying Pt3372 signal peptide was transferred into YPRAA. pSUC2-SP3372 showed that only the signal peptide had secretory function could grow normally in YPRAA. **b** The Pt3372 ORF sequence and the ORF sequence without the signal peptide were fused in-frame to the invertase sequence in the pSUC2 vector. The pSUC2-Pt3372 and pSUC2-Pt3372$^{\Delta SP}$ were used to indicate that only the yeast strain capable of secreting invertase could react with 2,3,5-triphenyl tetrazolium chloride (TTC) and reduce it to insoluble red 1,3,5-triphenyl formazan (TPF)

is localized in the nucleus and cell membrane (Fig. 3a). Western blot (WB) showed that the fusion protein Pt3372-GFP could be expressed normally in *N. benthamiana* (Fig. 3b).

Pt3372 inhibits programmed cell death in *N. benthamiana* and wheat

BAX (pro-death protein of the Bcl-2 family in mice) (Lacomme and Santa 1999), and INF1 (PAMP factor from *Phytophthora infestans*) (Kamoun et al. 1998) could trigger programmed cell death (PCD) when expressed in tobacco. To clarify the virulence function of Pt3372, we used the *Agrobacterium*-mediated PVX expression system (pGR107 vector) to express the recombinant vector PVX:Pt3372 and the negative control PVX:GFP in *N. benthamiana*. GV3101 strains carrying PVX:BAX was infiltrated into *N. benthamiana* at the same site 24 h post infiltration of PVX:Pt3372. The phenotype was observed 5 d later. The results showed that the bacterial suspension carrying PVX:GFP and PVX:Pt3372 did not induce cell death, but an obvious necrotic spot appeared at the PVX:BAX site. On the contrary, no obvious necrotic spots were found at the site of infiltration of PVX:Pt3372 and PVX:BAX, indicating that Pt3372 can inhibit the necrosis induced by BAX (Fig. 4a). Subsequently, we used the same method and observed that it can inhibit the necrosis induced by INF1 (Fig. 4b). Altogether, the results demonstrate that *Pt3372* has a virulent function.

The T3SS is an important 'weapon' for most Gram-negative pathogenic bacteria for successful colonization of their host (Thomas et al. 2009). Our goal was to deliver a putative suppressor using *P. fluorescens* EtHAn and defense-inducing effectors using *Pst* DC3000, the bacterium that causes tomato speck. However, when a syringae is inserted into wheat, *Pst* DC3000 produces a hypersensitive reaction (HR) (Yin and Hulbert. 2011). In order to clarify the function of Pt3372 in pathogenicity, *Pt3372* was transiently expressed in wheat cultivar Thatcher by bacterial T3SS. The results showed that *Pst* DC3000 induced HR on Thatcher, but pEDV6-Pt3372 and pEDV6 could not (Fig. 4c). HR reaction occurred at the infiltration site of pEDV6 & *Pst* DC3000, which was consistent with the symptoms of *Pst* DC3000 infiltration alone, while HR did not occur at the co-infiltration site of pEDV6-*Pt3372* & *Pst* DC3000. These results clearly demonstrate that Pt3372 inhibits the cell death induced by *Pst* DC3000 and plays a toxic role in wheat.

Pt3372 decreases the callose deposition, ROS accumulation, and expression of defense-related genes in TcLr2a and TcLr18

It was reported that *P. fluorescens* strain EtHAn can promote callose deposition in wheat and trigger the PTI reaction (Yin and Hulbert 2011). The empty vector pEDV6 was used as a negative control, and samples were collected at 24 and 48 hpi, respectively. We found that the EtHAn:pEDV6 induced callose

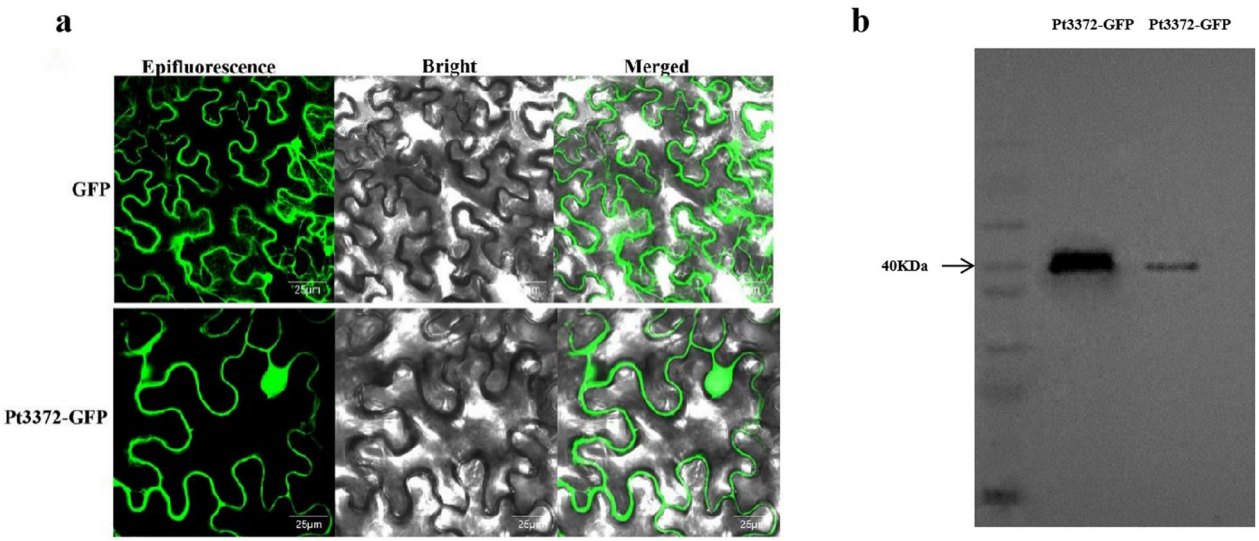

Fig. 3 The effector protein Pt3372 is localized in the nucleus and cell membrane. **a** The GFP and Pt3372-GFP fusion constructs were transformed into *Agrobacterium* and infiltrated into tobacco leaf tissues at 4–6 weeks of age. Scale bar: 25 μm. The epidermis of *N. benthamiana* leaves was removed and soaked in 0.8 M mannitol to achieve the purpose of plasmolysis. Fluorescence microscope (Leica, Germany) was used to observe the expression level and localization of effector proteins. **b** Pt3372 could be expressed in tobacco cells, which was detected by Western Blot. The protein concentration in the first lane was 50 μg. The protein concentration in the second lane was 10 μg

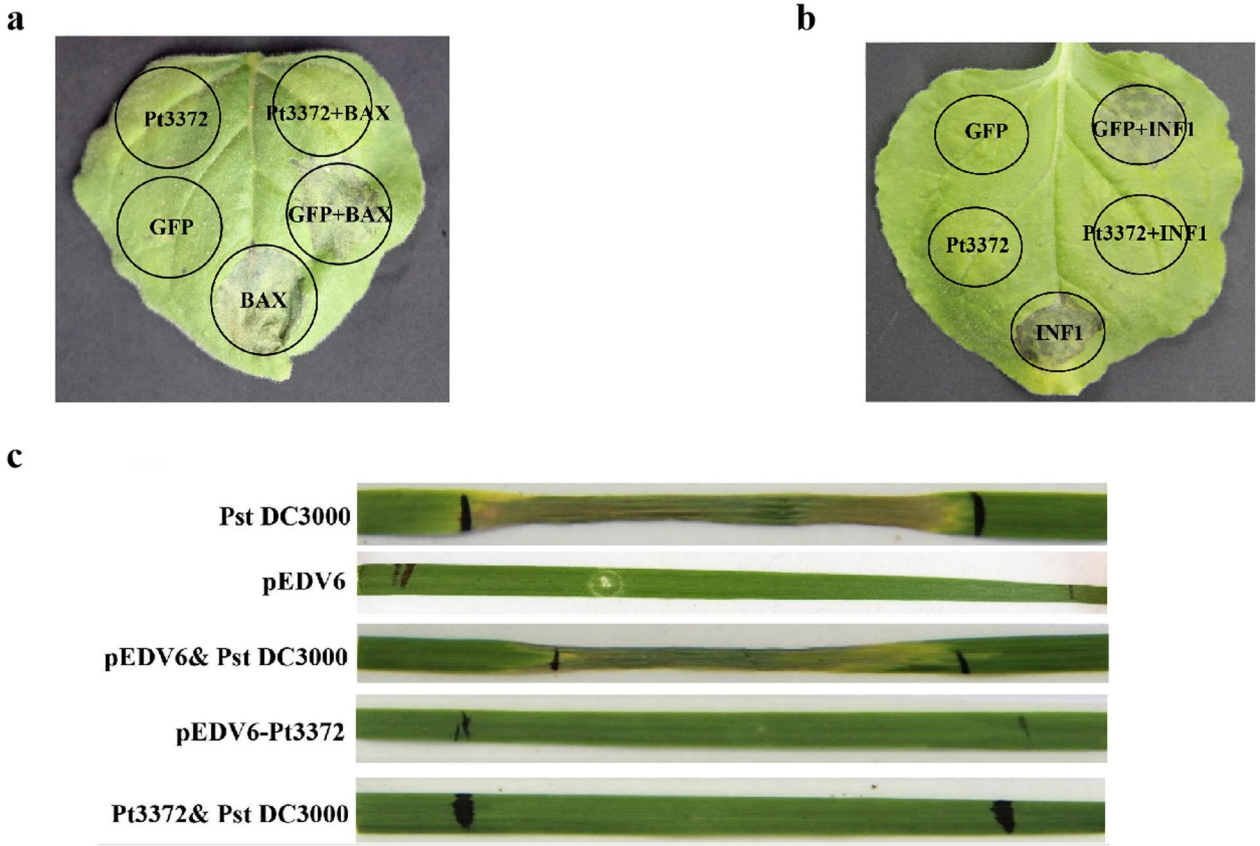

Fig. 4 Pt3372 inhibits programmed cell death (PCD) induced by BAX, INF, and *Pst* DC3000. **a**, **b** *Agrobacterium tumefaciens* GV3101 carrying PVX:Pt3372 and PVX:GFP was infiltrated into tobacco leaves, and PVX:BAX or PVX:INF1 was infiltrated at the same position 24 h later. BAX and INF1 caused cell death 24 h after infiltration of *A. tumefaciens* carrying PVX:Pt3372. **c** Pt3372 was transferred into two-leaf wheat Thatcher by *Pseudomonas fluorescens* EtHAn, which could not cause necrosis in wheat but could inhibit the necrosis induced by *Pst* DC3000. pEDV6 was used as a control. Photographs were taken 5 d post infiltration

deposition in wheat near-isogenic lines TcLr2a and TcLr18 (Fig. 5), which gradually increased with time, indicating that pEDV6 does not affect the role of EtHAn. EtHAn:Pt3372 also induced callose deposition in TcLr2a (Fig. 5a, b) and TcLr18 (Fig. 5c, d). However, compared with pEDV6, Pt3372 significantly inhibited callose deposition in TcLr2a (Fig. 5b) and TcLr18 (Fig. 5d).

qPCR was used to detect whether transient expression of Pt3372 could inhibit the expression of *TaPR1* and *TaPR2* genes related to wheat immune response. The results showed that the transient expression of Pt3372 suppressed the expression of *TaPR1* and *TaPR2* in TcLr2a (Additional file 1: Figure S1a, b) and TcLr18 (Additional file 1: Figure S1c, d). We also further analyzed the effect of JHKT inoculation on ROS accumulation in wheat. The results showed that EtHAn:Pt3372 significantly suppressed H_2O_2 accumulation in TcLr2a (Fig. 5e, f) and TcLr18 at 24 h and 48 h post-inoculation (Fig. 5g, h). These findings demonstrate that Pt3372 inhibited callose deposition, ROS accumulation, and expression of defense-related genes in TcLr2a and TcLr18.

Pt3372 silencing reduces *Pt* virulence in TcLr2a and TcLr18

Pt3372 was silenced by the BMSV-mediated HIGS approach (Cheng et al. 2017). The primers (Additional file 2: Table S1) were designed to select 250–300 bp as the silencing target (Additional file 1: Figure. S2a). The *Agrobacteria* carrying all the constructs were infiltration into *N. benthamiana* leaves. After the 'mosaic' virus spot appeared (Additional file 1: Figure S2b), the leaves were ground into homogenate, and the wheat near-isogenic lines TcLr2a and TcLr18 were inoculated. Mild yellowing symptoms were observed 14 d after inoculation (Additional file 1: Figure S2d–f). After that, *Pt* race JHKT was inoculated on the third leaf of wheat, and the phenotype was observed and photographed after 12 d (Fig. 6a, b). Phenotypic observations showed that after silencing *Pt3372*, the pathogenicity of JHKT in TcLr2a and TcLr18 was significantly reduced compared to the control

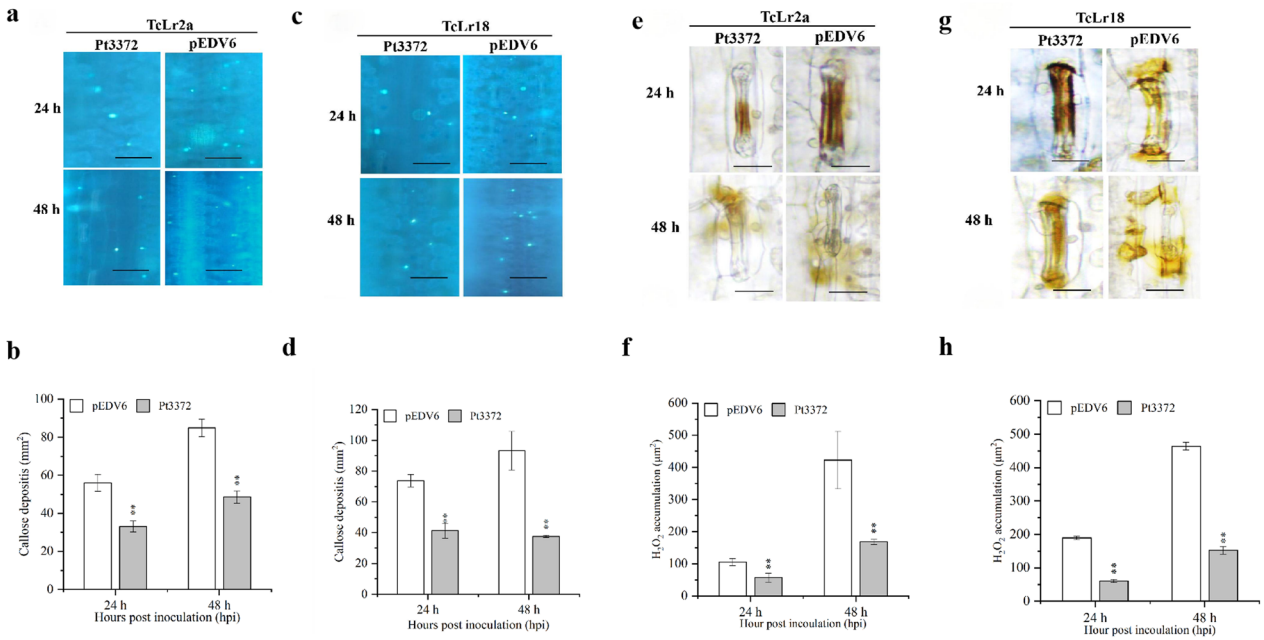

Fig. 5 Pt3372 inhibits callose deposition and reactive oxygen species in wheat TcLr2a and TcLr18. **a–d** The second leaf of TcLr2a and TcLr18 were inoculated with EtHAn carrying pEDV6-Pt3372 and pEDV6. At 24 and 48 hpi, the wheat leaves were stained with 0.5% aniline blue, and callose deposition was observed by fluorescence microscope. The software Image-Pro Plus 6.0 was used to calculate the average callose deposition per mm^2 in wheat leaves. **e–h** The average amount of H_2O_2 accumulation in wheat leaves inoculated with pEDV6-Pt3372 and pEDV6 per μm^2 at 24 and 48 hpi. The bar chart represents the mean (± SE) of three independent biological replicates, with 15 per unit area per replicate. Differences were detected using the unpaired two-tailored Student's t-test.Asterisks indicated significant difference (** $p < 0.01$, * $p < 0.05$), Scale bar: 20 μm

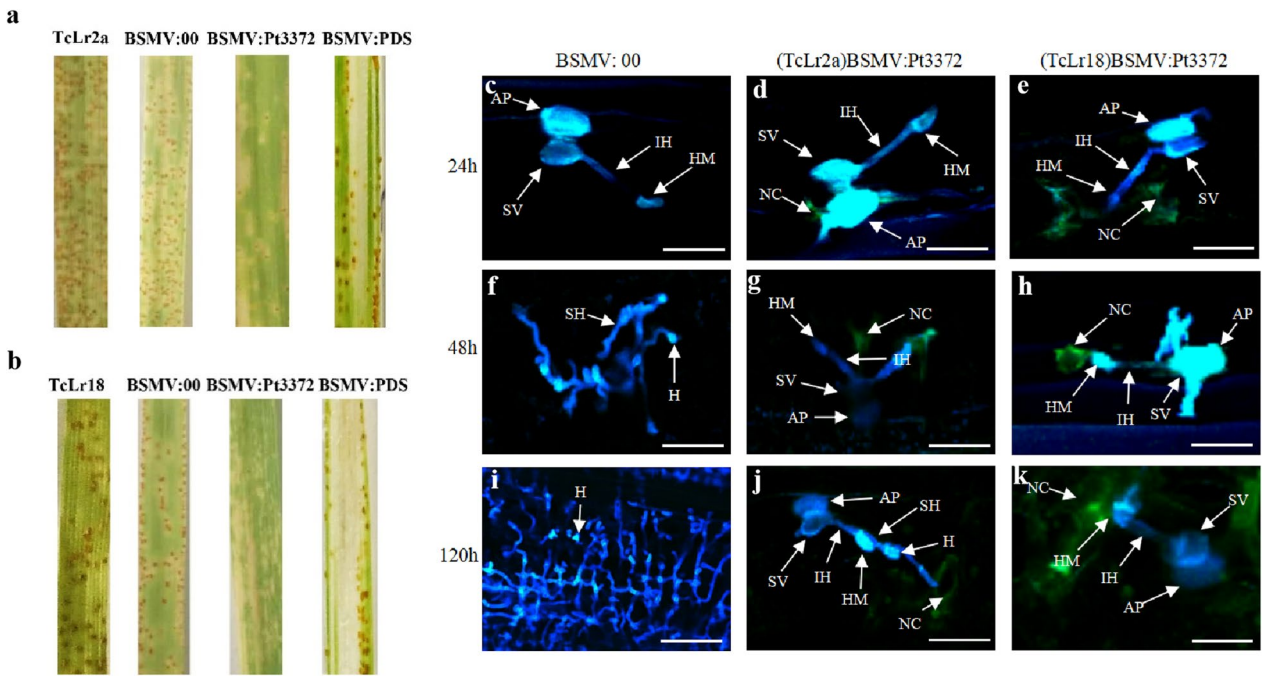

Fig. 6 Silencing of Pt3372 reduced JHKT virulence. **a**, **b** Phenotypes of the three leaves of TcLr2a and TcLr18 of silencing Pt3372 inoculated with *Pt* race JHKT at 14 dpi. **c**–**k** Histological observation of *Pt* JHKT inoculated on wheat TcLr2a and TcLr18 after BSMV infection, BSMV:00 represents the control group (empty vector-inoculated plants), while BSMV:Pt3372 denotes the experimental group with targeted Pt3372 gene silencing. (AP: appressorium; IH: primary mycelium; SV: substomatal vesicle; HMC: haustorial mother cell; H: haustorium; SH: secondary hyphae; NC: necrotic cells; Scale bar: 30 μm)

(infection type '3'). Infection types were recorded according to the 6-level grading method of Roelfs (1984), which included 0, 1, 2, 3, 4. 0–2 is low infection type, 3–4 is high infection type. In TcLr2a, the necrosis occurred accompanied by uredinium pile formation, and the infection type was '1' (Fig. 6a). TcLr18 showed necrosis only after inoculation with BSMV:*Pt3372* and JHKT, with infection type ';' (Fig. 6b). Furthermore, qPCR was used to analyze *Pt3372* expression level at 120 hpi with *Pt*. Compared with the control (BSMV:00), *Pt3372* expression was significantly decreased in TcLr2a and TcLr18 inoculated with BSMV:*Pt3372* (Additional file 1: Figure S2g), indicating the effective silencing of *Pt3372* in TcLr2a and TcLr18 plants.

The growth and development of *Pt* and host HR after inoculation with the virus were observed under a laser confocal microscope. *Pt* uredospores germinated to form appressorium, substomatal vesicle, primary hyphae, and haustorial mother cells in BSMV:00 at 24 hpi (Fig. 6c); however, it germinated to form appressorium, substomatal vesicle, primary hyphae, and haustorial mother cells, and necrosis occurred in BSMV:Pt3372 (TcLr2a) and BSMV:Pt3372 (TcLr18) (Fig. 6d, e) at the same time. At 48 hpi, *Pt* continued to grow, forming secondary hyphae and haustoria in BSMV:00 treatment (Fig. 6f), while forming only appressorium, substomatal vesicle, primary hyphae, and haustoria mother cells with necrosis in BSMV:Pt3372 (TcLr2a) and BSMV:Pt3372 (TcLr18) treatment (Fig. 6g, h). At 120 hpi, the hyphae continued to expand in BSMV:00 (Fig. 6i). At this time, secondary hyphae and haustorium were formed in BSMV:*Pt3372* (TcLr2a), and accompanied by a large amount of necrosis at the haustorium (Fig. 6j). However, fungal hyphae growth was still the same as that at 24 and 48 hpi and had only appressorium, substomatal vesicle, primary hyphae, and haustorium mother cells with green necrosis (Fig. 6k) in BSMV:Pt3372 (TcLr18). Based on the phenotypic and histopathological observation, it was speculated that *Pt3372* silencing may inhibit the growth and development of fungal hyphae. We therefore concluded that Pt3372 plays a virulence role during the *Pt* infection in TcLr2a and TcLr18.

Overexpression of *Pt3372* suppresses wheat resistance to leaf rust

To further confirm the role of *Pt3372* during leaf rust infection, we generated *Pt3372* overexpressing (*Pt3372*-6E) transgenic plants with spring wheat cv. Fielder and selected positive lines in T_1 generation for disease resistance identification. PCR detection showed that both transgenic lines L1 and L7 contained the *Pt3372* gene (Fig. 7a). *Pt* race JHKT was inoculated on two-leave stage transgenic plants, and samples were collected at 24 and 48 hpi for RT-PCR. The results showed that the overexpression lines L1 and L7 had uredinium on the leaves, accompanied by necrosis or chlorosis around the uredinium, showing susceptibility (Fig. 7b). However, the wild-type wheat (WT, Fielder) showed resistance to JHKT, and no obvious infection court and necrosis appeared on the leaves (Fig. 7b). These results demonstrated that overexpression of *Pt3372* attenuated the resistance of Fielder to leaf rust; thus, Pt3372 presented a virulence function. In addition, qPCR results showed that in the overexpression lines L1 and L7, wheat pathogenesis-related gene *TaPR2* (Fig. 7c) and glutathione reductase *TaGR* (Fig. 7f) were downregulated, while wheat superoxide dismutase *TaSOD* (Fig. 7d) and catalase genes *TaCAT* (Fig. 7e) were upregulated, indicating that Pt3372 could promote *Pt* infection by interfering with the expression of wheat PR and protective enzymes encoding genes.

Pt3372 targets wheat elicitor responsive protein 3 (TaERP3)

To identify wheat proteins that interact with Pt3372, Pt3372 without signal peptide sequence was used as a bait to screen a yeast-two-hybrid (Y2H) library constructed from wheat leaves infected by *Pt* from which several candidate target proteins were identified, including Elicitor-responsive protein 3 (TaERP3). Sequence analysis showed that TaERP3 contains a C2 domain (Additional file 1: Figure S3a). By blasting the TaERP3 sequence against the hexaploid wheat genome database (http://plants.ensembl.org/index.html), three copies of TaERP3 located on chromosomes 2A, 2B, and 2D, respectively, were matched (Additional file 1: Figure S3b). In this study, the TaERP3 sequence was located on chromosome 2D in the wheat cultivar Thatcher. *TaERP3* was induced in the early stage of *Pt* infection (Additional file 1: Figure S4a, b) and was localized in the nucleus and cell membrane (Additional file 1: Figure S4c). WB detection showed that TaERP3—GFP protein could be normally expressed (Additional file 1: Figure S4d).

The coding sequence of *Pt3372* and the open reading frame of *TaERP3* were cloned into the vectors pGBKT7 and pGADT7, respectively, to confirm the interaction between Pt3372 and TaERP3. pGBKT7-Lam & pGADT7-T, and pGBKT7-53 & pGADT7-T were used as negative and positive controls, respectively. The results showed that pGBKT7-Pt3372 & pGADT7-TaERP3 can grow normally on SD/-Trp/-Leu/-His/-Ade medium containing X-α-gal (Fig. 8a), and the interaction between Pt3372 and TaERP3 was further confirmed by BiFC (Fig. 8b) and Co-IP assays (Fig. 8c).

To further clarify the regions essential for the interaction of Pt3372 with TaERP3, we generated a Pt3372 mutant (Additional file 1: Figure S5a) and three TaERP3 deletion mutants (Additional file 1: Figure S5b) by amino

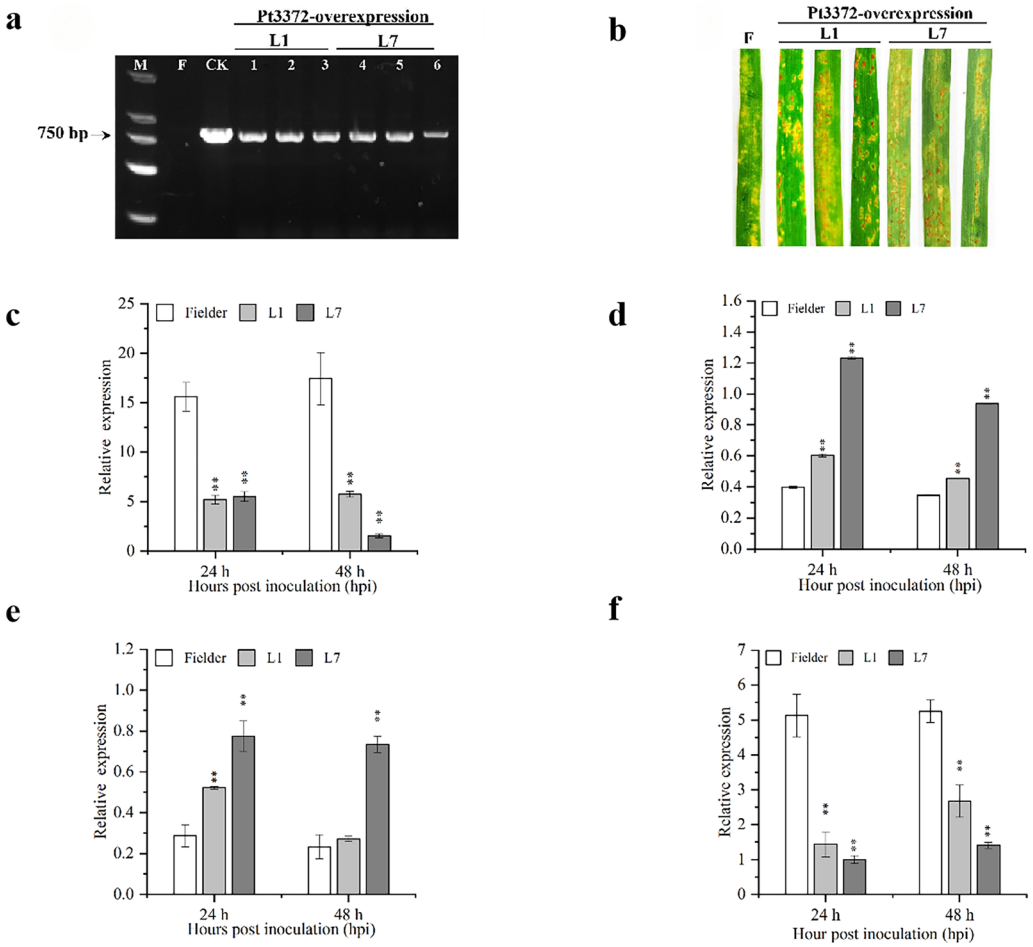

Fig. 7 Effect of overexpression of Pt3372 on disease resistance of wheat. **a** PCR identification of T1 generation Pt3372 overexpressing transgenic plants, with the recombinant vector pANIC6E-Pt3372 as the positivity control (CK), Wild Fielder was used as a negative control (F). **b** Phenotypic identification of transgenic plants after inoculation with JHKT, and phenotypic observation and photographing were performed 14 dpi after inoculation. **c**–**f** The transcription levels of *TaPR2*, *TaSOD*, *TaCAT*, and *TaGR*, respectively, in transgenic materials at 24 h and 48 h after inoculation, and the values were the mean ± SE of the three independent samples (*: $p < 0.05$; * *: $p < 0.01$)

acid deletion approach. The results showed that the Pt3372$^{\Delta SP}$ mutant lacking 20 aa at the N-terminal could not interact with TaERP3, Pt3372 could interact with TaERP3, and TaERP3 mutant 3 (1–60 aa) lacking 60 aa at the N-terminus of C2 structure could not interact with Pt3372 (Additional file 1: Figure S6). Mutants 1 and 2 that only retain the C2 domain and the N-terminal deletion of 30 aa of the C2 structure interacted with Pt3372. Therefore, it was inferred that 1–20 aa adjacent to the signal peptide at the N-terminal of Pt3372 interacts with the C2 domain of TaERP3, with the 30–60 aa of the C2 domain being critical for the interaction.

Discussion

Pt3372 is a virulence effector

Plant pathogens, including bacteria, oomycetes, and fungi, secrete various proteinaceous and non-proteinaceous effectors to suppress the host immune system and facilitate colonization. Effector proteins are very small in size (less than 300 aa), rich in cysteine, have no transmembrane domain and no known conserved Pfam domain, and are highly expressed in the haustoria or infection cycle (Catanzariti et al. 2007; Jaswal et al. 2020; Xu et al. 2020; Pradhan et al. 2021; Waheed et al. 2022; Zhang et al. 2022). The N-terminal of the effector proteins PSTha5a23 and Pst_8713 from stripe rust with typical signal peptides, which were rich in cysteine and highly expressed in the early stage of infection, and play virulence functions in the infection process of stripe rust (Cheng et al. 2017; Zhao et al. 2018). In this study, we identified a *Pt* effector, Pt3372, which is a small protein possessing a signal peptide with a secretory function. Pt3372 showed virulence on the plant with inhibition of the BAX/INF1-induced PCD in *N. benthamiana* (Fig. 4a,

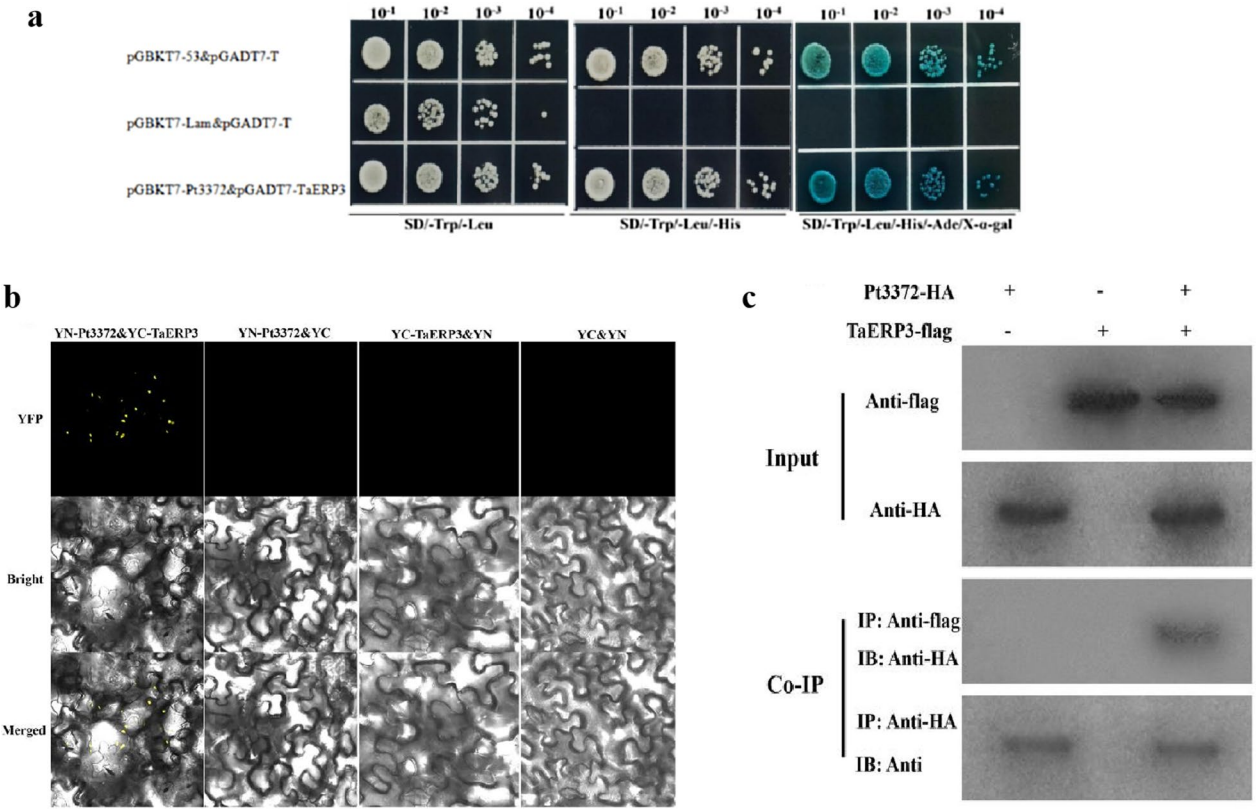

Fig. 8 Pt3372 interacts with TaERP3. **a** The interaction between Pt3372 and TaERP3 was verified by yeast two-hybrid. The recombinant plasmids pGBKT7-Pt3372 and pGADT7-TaERP3 were co-transformed into Y_2Hgold, and the clones were sampled and diluted to 10^{-1},10^{-2},10^{-3}, and 10^{-4}, respectively. The clones were cultured on the selective medium SD/-Trp/-Leu, SD/-Trp/-Leu/-His, and SD/-Trp/-Leu/-His/-Ade/-X-α-gal, with pGBKT7-Lam & pGADT7-T and pGBKT7-53 & pGADT7-T as negative and positive controls, and photographed after 3 d of culture. **b** The interaction between pGBKT7-Pt3372 and pGADT7-TaERP3 was detected by BiFC assay. Pt3372 and TaERP3 were constructed into vectors pEarleyGate201-YN and pEarleyGate202-YC, respectively. YN-Pt3372 & YC-TaERP3, YN-Pt3372 & YC, YC-TaERP3 & YN and YC & YN were mixed in a ratio of 1: 1 and infiltrated into tobacco. After 3 d of culture, laser confocal microscope observation was used, Scale bars: 25 μm. **c** Co-IP was used to verify the interaction between pGBKT7-Pt3372 and pGADT7-TaERP3 in vivo. The leaf proteins of *N. benthamiana*, which simultaneously expressed Pt3372-HA and TaERP3-Flag, were extracted for co-immunoprecipitation (Co-IP). Pt3372-HA and TaERP3-Flag were detected by HA antibody and Flag antibody Western blot, respectively

b) and PCD induced by *Pst* DC3000 in wheat (Fig. 4c). Pt3372 also inhibited callose deposition and ROS accumulation (Fig. 5) in TcLr2a and TcLr18.

The use of an *Agrobacterium*-mediated genetic transformation system to generate transgenic materials containing pathogenic factors is a robust means to study the function of effector proteins. For example, *PstGSRE4* transgenic wheat reduced wheat resistance to stripe rust, significantly increased the number of urediospores of stripe rust and inhibited ROS accumulation and callose deposition (Liu et al. 2022). Furthermore, *Pst27791* transgenic wheat enhanced pathogen virulence and reduced wheat resistance to *Pst*. Obvious urediospores on wheat leaves were observed, and it suppressed ROS accumulation and expression of wheat defense-related genes (Wan et al. 2022). To verify the virulence of *Pt3372* on wheat, a *Pt3372* transgenic line was generated, and obvious uredinium appeared on wheat leaves after *Pt* inoculation, which downregulated the expression of wheat defense-related genes *TaPR2* and glutathione reductase *TaGR* (Fig. 7f), while wheat superoxide dismutase and catalase genes *TaSOD* (Fig. 7d) and *TaCAT* (Fig. 7e) were upregulated. *TaPR2* encodes β-1,3-glucan endonuclease, with enzymatic activity, which can weaken and digest the fungal cell wall. As an important member of antioxidant enzymes in plants, glutathione reductase TaGR can reduce oxidized glutathione disulfide (GSSG) to reduced glutathione (GSH), thus providing reducing power for the removal of ROS, protecting plants from harm. *TaPR2* and glutathione reductase *TaGR* were downregulated indicating that *Pt3372* plays a virulence role during the process of *Pt* infection (Fig. 7). At the same time, wheat superoxide dismutase and catalase genes *TaSOD* (Fig. 7d) and *TaCAT* (Fig. 7e) were upregulated in *Pt3372* transgenic

line, indicating an increased ability to remove ROS. These results once again demonstrate that overexpression of *Pt3372* enhanced *Pt* virulence and suppressed wheat immunity.

Pt3372 is virulent in TcLr2a and TcLr18

The accumulation of reactive oxygen species is one of the early features of plant defense response and plays a key role in the immune system (Coll et al. 2011). Inhibition of ROS accumulation is an important strategy for successful infection and colonization of obligate parasitic pathogens (Liu et al. 2022). For instance, the effector proteins Pst18363, PstCFEM1, and Pst_8713 inhibited callose deposition and ROS accumulation in wheat and promoted pathogen infection (Zhao et al. 2018; Yang et al. 2020; Bai et al. 2022). Herein, we confirmed that Pt3372 can inhibit callose deposition and ROS accumulation in TcLr2a and TcLr18, and promotes *Pt* infection, demonstrating that it is a key virulence factor.

HIGS, an RNA interference (RNAi)-based approach, has been developed for functional analysis and characterization of biotrophic fungal genes using BSMV in wheat (Yin and Hulbert 2011; Panwar et al. 2018). HIGS induced by BSMV-VIGS (virus-induced gene silencing) was established to be a robust, high-throughput approach for the functional analysis and validation of rust fungi candidate genes involved in pathogenicity through quantitative estimation of infection-related traits (Panwar et al. 2018; Yin and Hulbert 2018). BSMV-mediated HIGS silencing of the *Pt* effector Pt13024 in wheat near-isogenic line TcLr30 enhanced *Pt* infection, indicating that Pt13024 plays an avirulent function on TcLr30 (Qi et al. 2023). In this study, BSMV-mediated HIGS silencing of *Pt3372* in both TcLr2a and TcLr18 reduced the pathogenicity of *Pt* race JHKT, confirming that Pt3372 played a virulent role in TcLr2a and TcLr18 (Fig. 6). We will further explore the molecular mechanism of Pt3372 confers virulence to Lr2a and Lr18.

Pt3372 interacts with TaERP3

In this study, TaERP3 was identified as the target protein of Pt3372 (Fig. 8). TaERP3 is a plant C2 domain protein. The C2 domain of TaERP3 consists of 1–103 amino acids at the N-terminal and contains five aspartic acid (D) binding sites. C2 domain proteins are involved in plant growth, development, senescence, membrane localization, and abiotic and biotic stress responses, and play an important role in signal transduction and membrane transport pathways (Nalefski and Falke 1996; Kim et al. 2003; Schapire et al. 2008; Yokotani et al. 2009; Silva et al. 2011). The rice C2 domain gene *OsERG1* is involved in defense response and membrane translocation in a Ca^{2+}-dependent manner (Kim et al. 2003). *Arabidopsis* BAP and BON proteins negatively regulate disease-resistance gene-mediated defense responses and can also inhibit PCD (Yang et al. 2007). *Brassica* IPG-1 participates in host PCD in a Ca^{2+}-dependent manner (Wang et al. 2009). Therefore, we speculated that TaERP3 may bind to Ca^{2+} and participate in host defense responses. It was found that wheat elicitor responsive gene 3 (*TaERG3*) was highly induced during the compatible and incompatible interaction between wheat and stripe rust (Zhang et al. 2013). It was also established that it is localized in the plasma membrane and nucleus of onion epidermal cells and may participate in the defense response of wheat to stripe rust through ABA-dependent signaling pathways (Zhang et al. 2013). TaERP3, the Pt3372 target protein obtained in this study, was highly expressed in the early stage of the compatible and incompatible interactions between *Pt* and wheat (Additional file 1: Figure S4a, b). It was found to be localized throughout the whole cell of tobacco (Additional file 1: Figure S4c), so we speculated that it may also be involved in ABA-dependent signaling pathways. However, the detailed function of TaERP3 will be further explored.

The interaction between Pt3372 and TaERP3 was confirmed using the amino acid deletion method (Additional file 1: Figure S6). Silencing *Pt3372* through HIGS effectively reduced *Pt* virulence, indicating a positive correlation between the interaction target and disease resistance. Therefore, overexpressing interaction targets can be utilized to modify the interaction site of wheat TaERP via gene editing, thereby preventing *Pt* invasion. This approach has the potential to develop durable wheat leaf rust-resistant cultivars; however, further research is required to investigate the functional aspects of this target. It should be noted that there is a high similarity (99.54%) in TaERP3 protein sequence among 2A, 2B, and 2D, and there are differences in 15 aa and 130 aa (Additional file 1: Figure S3c). The identified interaction domain between Pt3372 and TaERP3 corresponds to the 30–60 aa of the C2 domain. Hence, we speculated that different alleles of TaERP3 may have varying effects on the regulation of wheat immunity, which warrants future investigation.

Conclusion

Pt3372 is a *Pt* effector protein of 139 aa, with a signal peptide of 1–24 aa at the N-terminal. It showed virulence by inhibiting PCD induced by BAX and INF1 in *N. benthamiana* and *Pst* DC3000 in wheat. Pt3372 can suppress callose deposition and ROS accumulation in wheat near-isogenic lines TcLr2a and TcLr18 by interacting with wheat TaERP3 on chromosome 2D. Overexpression of *Pt3372* increased pathogen virulence and reduced

wheat resistance to *Pt* JHKT, whilst silencing *Pt3372* reduced pathogen virulence in TcLr2a and TcLr18. Altogether, our results indicate that Pt3372 suppresses wheat immunity by targeting TaERP3 in TcLr2a and TcLr18.

Methods

Plant materials and strains

Wheat near-isogenic lines TcLr2a and TcLr18 were used to quantitatively analyze and observe callose deposition and ROS accumulation, and Pt3372 pathogenicity function analysis by HIGS. The common wheat cultivar Zhengzhou 5389 was used for the propagation of leaf rust fungus, and Fielder was used for the generation of transgenic lines. *Nicotiana benthamiana* and *Agrobacterium* GV3101 were used for the transient expression of Pt3372. Wheat and *N. benthamiana* were sowed and maintained in a greenhouse at 22 ± 2 °C with 16 h of light and 8 h of darkness. Transient expression analysis was performed using *N. benthamiana* plants aged 4–6 weeks. *Pseudomonas fluorescens* EthAn (effector-to-host analyzer) and *Pseudomonas syringae* pv. tomato DC3000 (*Pst* DC3000) were used for T3SS-mediated overexpression of Pt3372. Yeast strain YTK12 was used for validation of signal peptide secretory function, and Y_2H Gold was used for yeast two-hybrid assay. High virulent *Pt* race JHKT (13-5-28-1) was used for HIGS and Pt3372 overexpression analysis.

Bioinformatic analysis of Pt3372

To analyze whether Pt3372 is a secretory effector protein (SEP), online server such as SignalPv4.1 (http://www.cbs.dtu.dk/services/SignalP/), TargetPv1.1 (http://www.cbs.dtu.dk/services/TargetP/), TMHMMv2.0 (transmembrane prediction using hidden Markov models) (http://www.cbs.dtu.dk/services/TMHMM/), Pfam (http://pfam.xfam.org/), SOPMA (self-optimized prediction method with alignment) (http://npsa-pbil.ibcp.fr/cgi-bin/npsa_automat.pl?Page=npSA_sopma.html) were used to analyze the Pt3372 sequence (Qi et al. 2023), and UniProt (https://www.uniprot.org/blast) was used to analyze the TaERP3 protein domain.

qRT-PCR analysis of *Pt3372*

Wheat leaves were collected at 0 (urediniospores, US), 6, 12, 18, 24, 36, 72, 96, 120, 144, 216, and 288 h post inoculation (hpi) with JHKT. Total RNA was extracted from all samples using the UNlQ-10 Column Trizol Total RNA Isolation Kit (Biotechnology China, Shanghai, B511321). Single-stranded cDNA was synthesized by reverse transcription using 5×All-In-One RT MasterMix (ABM, China, Shanghai, G490). After dilution, 1 μL of the synthesized cDNA was used for qRT-PCR, and the specific primers used are shown in Additional file 2: Table S1. *PtActin* was used as the internal reference gene for the expression analysis of related genes in *Pt*. The relative expression of the gene was calculated according to the $2^{-\Delta\Delta CT}$ method (Livak and Schmittgen 2001), and repeated three times. Student's *t*-test was used to evaluate the statistical significance.

Secretory function analysis of Pt3372 signal peptide

The yeast secretion trap systems and 2,3,5-triphenyltetrazonium chloride (TTC) color reaction were used to verify the secretory function of the Pt3372 signal peptide (Jacobs et al. 1997; Oh et al. 2009; Yin et al. 2018). Pt3372 signal peptide was cloned into the vector pSUC2T7M13ORI (pSUC2) using specific primers indicated in Additional file 2: Table S1 and transformed into the invertase mutant yeast strain YTK12. The positive transformants were screened on SD/-Trp (Shaanxi Puind Bioengineering Co., Ltd., China, Shaanxi, PT1050). The positive transformants and the negative and positive controls were then diluted according to the ratio of 1:1, 1:10, 1:100, and spot cultured on YPRAA medium (1% yeast extract, 2% peptone, 2% raffinose, 2 μg/L antimycin A, and 2% agar), YPDA (1% yeast, 2% peptone, 2% glucose, 0.003% adenine sulfate, 2% agar and SD/-Trp, respectively (Zhao et al. 2018). The enzyme activity of the invertase was detected through its ability to reduce TTC to insoluble red 1,3,5-triphenylformic acid (TPF).

Agrobacterium-mediated transient assay

The *A. tumefaciens* strain GV3101 carrying vectors was grown overnight in Luria–Bertani (LB) medium supplemented with 50 μg/mL kanamycin and 50 μg/mL rifampicin. The subcellular localization and toxicity analysis of Pt3372 in tobacco was performed as described by Qi et al. (2023).

Bacterial T3SS-mediated *Pt3372* overexpression in wheat

According to the method by Qi et al. (2023), the EtHAn (carrying an empty vector pEDV6 and pEDV6-Pt3372) were cultured, infiltrated into wheat, and samples were collected to detect callose deposition. For reactive oxygen species accumulation detection, wheat leaves were placed in 0.01% 3,3′-Diaminobenzidine (DAB) staining solution, irradiated under strong light for 8 h, and then decolorized with 95% ethanol until the leaves became white. The ROS were observed under a microscope (bright field) and photographed. The callose deposition and reactive oxygen species accumulation were statistically analyzed using ImageJ software. Subsequently, qRT-PCR was used to analyze the expression patterns of *TaPR1*, *TaPR2*, *TaSOD*, *TaCAT*, and *TaGR* in wheat, using *TaGAPDH* as the internal reference gene. For phenotypic observations,

the collected EtHAn (pEDV6 and pEDV6-Pt3372) were diluted to $OD_{600}=1.0$, *Pst* DC3000 strain $OD_{600}=0.4$, and *Pst* DC3000 strain was co-infiltrated into the second leaf of wheat in a ratio of 1:1, this experiment was repeated three times, and the phenotype was observed and photographed after 3–5 days (Xu et al. 2019).

Barley stripe mosaic virus (BSMV)-mediated gene silencing

The specific fragment of *Pt3372* was ligated into the BSMV-γ vector to construct the recombinant vector BSMV:*Pt3372*, which was then transformed into *Agrobacterium* EHA105 according to the method by Qi et al. (2023). BSMV infected tobacco leaves were harvested and ground in 1% celite in 0.1 M PB buffer (pH 7.4) (Coolaber), and gently rubbed with gloved fingers onto the second leaf of the wheat seedlings. The virus-treated seedlings were maintained at 22 ± 2 °C for 15 d in the greenhouse. The fresh *Pt* race JHKT was inoculated using the smearing method. After 16 h of darkness and 100% moisture retention, it was transferred to a 22 ± 2 °C light greenhouse for normal culture. Leaf samples were collected at 24, 48, and 120 hpi for RNA extraction. The silencing efficiency of BSMV-*Pt3372* was detected by qRT-PCR, and histopathological observation of the growth and development of *Pt* after silencing *Pt3372* was observed under a microscope. The phenotype of the third leaf was observed and photographed after 14 d, according to Qi et al. (2023).

Overexpression of *Pt3372* in fielder

The *Pt3372* ORF was constructed into the wheat transgenic vector pANIC6E by Gateway technology, and the recombinant vector pANIC6E-Pt3372 was transformed into EHA105. The positive monoclonal was sent to the transgenic platform of the Key Laboratory of Crop Adversity Biology in Arid Areas of Northwest A & F University. The exogenous gene *Pt3372* was introduced into wheat Fielder to obtain the wheat transgenic line *Pt3372*-6E. The inserted fragments were detected by PCR to screen positive transgenic plants. When the *Pt3372*-6E T1 generation grew to the second leaf, it was inoculated with *Pt* race JHKT, and RNA samples were collected at 24 h and 48 h for the analysis of disease-related gene expression. The phenotype was recorded on 14 dpi.

Yeast two-hybrid test

The cDNA library was constructed from the leaves of wheat Thatcher infected with *Pt* race JHKT at 0, 6, 12, 24, 36, 48, 72, 96, 120, 144, and 216 hpi, respectively. Using pGBKT7-Pt3372 as the bait, the interaction protein of Pt3372 was screened according to Liu et al. (2022). In order to clarify the interaction region between Pt3372 and TaERP3, the mutants of Pt3372 and TaERP3 were constructed by the amino acid deletion method, and the interaction was verified by co-transformation.

Co-IP and BiFC assay

The GV3101 strain carrying YN-Pt3372 and YC-TaREP3 was cultured overnight at 28 °C, and the OD_{600} was adjusted to 0.5, mixed in a ratio of 1:1, and the mixture was infiltrated into 4-weeks-old *N. benthamiana* leaves. After 48 h, samples were collected, and 100 µL of co-infiltrated protein was extracted as a control (Input). 10 µL anti-HA-tag magnetic beads were added to the remaining extract, mixed upside down, incubated at 4 °C for 3 h, centrifuged at 5000 *g* for 30 s, and the supernatant was removed. The beads in the washing buffer with a volume of 60 µL were mixed with 20 µL of the loading buffer and heated at 100 °C for 5 min. The precipitated protein and crude protein (Input) were hybridized with anti-HA (Abcom, ab1424) and anti-Flag (Sihma, F1804) antibodies, respectively. After 2–3 d, the cells were observed under a laser confocal FV1000 microscope, and three biological replicates were set.

Western blotting

Proteins were separated by sodium dodecyl-sulfate polyacrylamide gel electrophoresis (SDS-PAGE). The gel was transferred to polyvinylidene difluoride (PVDF) membrane (PALL, BSP0161) by wet transfer method. The PVDF membrane was immersed in a blocking solution (TBST, 5% skimmed milk powder), incubated for 1 h at room temperature, and then washed three times. Anti-HA and anti-flag antibodies were diluted to 1:1000 added to the PVDF membrane, and incubated at room temperature for 3 h. After washing four times, the secondary antibody goat anti-mouse (1:10,000) was added to the PVDF membrane and incubated at room temperature for 1 h. After washing four times, the fluorescent substrate was added to react for 5 min and then exposed and photographed.

Statistical analysis of data

Statistical analysis was performed using IBM SPSS Statistics 23 (IBM SPSS Statistics, IBM Corporation, Armonk, New York, USA) software.

Abbreviations

BAX	Bcl2-associated X
HR	Hypersensitive response
INF1	*Phytophthora infestans* INF1
PCD	Programmed cell death
PR	Pathogenesis-related protein genes
Pst DC3000	*Pseudomonas syringac* pv. DC3000
Pt	*Puccinia triticina*
WB	Western blot

Supplementary Information

The online version contains supplementary material available at https://doi.org/10.1186/s42483-025-00332-6.

Additional file 1: Figure S1. Pt3372 can inhibit the expression of pathogenesis-related genes in 16 TcLr2a and TcLr18. **Figure S2.** Pt3372 silencing fragment, the phenotype of tobacco and wheat after BSMV and Silencing efficiency of Pt3372. **Figure S3.** Sequence analysis of TaERP3. **Figure S4.** Expression analysis and subcellular localization of TaERP3. **Figure S5.** Design of Pt3372 and TaERP3 deletion mutants. **Figure S6.** The interaction region between Pt3372 and TaERP3.

Additional file 2: Table S1. Primers used in this study.

Acknowledgements
We thank Prof Wenwen Sun of China Agricultural University for providing us with the Agrobacterium receptor strain EHA105. We would like to thank Prof Dawei Li of China Agricultural University for the vector pCaBS-γb:LIC (HIGS-mediated gene silencing). We also thank Northwest A&F University for cultivating transgenic plants and Academician Zhensheng Kang for providing us with EtHAn and pEDV6.

Author contributions
XW, HL, JL, and WY contributed to the design of the work. XW, JL, and YZ performed the experiments and analyzed the sequencing data. XW wrote the manuscript, JM and WY revised the manuscript. XW, JL, JM, NZ, LS, JC, RL, YZ, DL, and WY drafted the manuscript. All authors read and approved the submitted version.

Funding
The work was supported by the National Natural Science Foundation of China (32172367; 31571956); Natural Science Foundation of Hebei (C2024204135); Modern Agricultural Industry System of Wheat Industry in Hebei Province (HBCT2023010205); Xingtai Innovation Ability Promotion Plan Project (2023ZZ080).

Availability of data and materials
Not applicable.

Declarations

Ethics approval and consent to participate
Not applicable.

Consent for publication
All authors agree with the publication.

Competing interests
The authors declare that the research was conducted in the absence of any commercial or financial relationships that could be construed as a potential conflict of interest.

Received: 4 October 2024 Accepted: 4 March 2025
Published online: 27 May 2025

References

Abebe W. Wheat leaf rust disease management: a review. J Plant Pathol Microbiol. 2021;8(3):1–14.
Anderson JP, Gleason CA, Foley RC, Thrall PH, Burdon JB, Singh KB. Plants versus pathogens: an evolutionary arms race. Funct Plant Biol. 2010;37(6):499–512.
Bai XX, Peng H, Goher F, Islam MA, Xu SD, Guo J, et al. A candidate effector protein PstCFEM1 contributes to virulence of stripe rust fungus and impairs wheat immunity. Stress Biol. 2022;2(1):21.
Bi WS, Zhao SQ, Zhao JJ, Su JJ, Yu XM, Liu DQ, et al. Rust effector PNPi interacting with wheat TaPR1a attenuates plant defense response. Phytopathol Res. 2020;2(1):1–14.
Boller T, Felix G. A renaissance of elicitors: perception of microbe-associated molecular patterns and danger signals by pattern-recognition receptors. Annu Rev Plant Biol. 2009;60(1):379–406.
Catanzariti AM, Dodds PN, Ellis JG. Avirulence proteins from haustoria-forming pathogens. Fems Microbiol Lett. 2007;269(2):181–8.
Chang JY, Mapuranga J, Li RL, Zhang YD, Shi J, Yan HF, et al. Wheat leaf rust fungus effector protein Pt1641 is avirulent to TcLr1. Plants (Basel). 2024a;13(16):2255.
Chang JY, Mapuranga J, Wang XD, Dong HJ, Li RL, Zhang YD, et al. A thaumatin-like effector protein suppresses the rust resistance of wheat and promotes the pathogenicity of *Puccinia triticina* by targeting TaRCA. New Phytol. 2024b;244(5):1947–60.
Cheng YL, Wu K, Yao JN, Li SM, Wang XJ, et al. PSTha5a23, a candidate effector from the obligate biotrophic pathogen *Puccinia striiformis* f. sp. *tritici*, is involved in plant defense suppression and rust pathogenicity. Environ Microbiol. 2017;19(5):1717–29.
Coll NS, Epple P, Dangl JL. Programmed cell death in the plant immune system. Cell Death Differ. 2011;18:1247–56.
Cui ZC, Shen SS, Meng LS, Sun XZ, Jin YQ, Liu YX, et al. Evasion of wheat resistance gene *Lr15* recognition by the leaf rust fungus is attributed to the coincidence of natural mutations and deletion in *AvrLr15* gene. Mol Plant Pathol. 2024;25(7):e13490.
de Jonge R, van Esse HP, Kombrink A, Shinya T, Desaki Y, Bours R, et al. Conserved fungal LysM effector Ecp6 prevents chitin-triggered immunity in plants. Science. 2010;329(5994):953–5.
Geng HM, Zhang YJ, Qin Z, Wang S, Liu CS, Cui ZC, et al. *Puccinia triticina* effector Pt-1234 modulates wheat immunity by targeting transcription factor TaNAC069 via its C subdomain. Crop J. 2024. https://doi.org/10.1016/j.cj.2024.07.013.
Gupta P, Roy S, Nandi AK. MEDEA-interacting protein LONG-CHAIN BASE KINASE 1 promotes pattern-triggered immunity in *Arabidopsis thaliana*. Plant Mol Biol. 2020;103(1–2):173–84.
Huerta-Espino J, Singh RP, Germán S, Mccallum BD, Park RF, Chen WQ, et al. Global status of wheat leaf rust caused by *Puccinia triticina*. Euphytica. 2011;179(1):143–60.
Jacobs KA, Collins-Racie LA, Colbert M, Duckett M, Golden-Fleet M, Kelleher K, et al. A genetic selection for isolating cDNAs encoding secreted proteins. Gene. 1997;198(1–2):289–96.
Jaswal R, Kiran K, Rajarammohan S, Dubey H, Singh PK, Sharma Y, et al. Effector biology of biotrophic plant fungal pathogens: current advances and future prospects. Microbiol Res. 2020;241:126567.
Jones JDG, Dangl JL. The plant immune system. Nature. 2006;444(7117):323–9.
Kadota Y, Shirasu K, Zipfel C. Regulation of the NADPH oxidase RBOHD during plant immunity. Plant Cell Physiol. 2015;56(8):1472–80.
Kamoun S, van der Lee T, van den Berg-Velthuis G, de Groot KE, Govers F. Loss of production of the elicitor protein INF1 in the clonal lineage US-1 of *Phytophthora infestans*. Phytopathology. 1998;88(12):1315–23.
Kim CY, Koo YD, Jin JB, Moon BC, Kang CH, Kim ST, et al. Rice C2-domain proteins are induced and translocated to the plasma membrane in response to a fungal elicitor. Biochemistry. 2003;42:11625–33.
Kolmer JA. Tracking wheat rust on a continental scale. Curr Opin Plant Biol. 2005;8(4):441–9.
Kunze G, Zipfel C, Robatzek S, Niehaus K, Boller T, Felix G. The N terminus of bacterial elongation factor Tu elicits innate immunity in *Arabidopsis* plants. Plant Cell. 2004;16(12):3496–507.
Lacomme C, Santa CS. Bax-induced cell death in tobacco is similar to the hypersensitive response. Proc Natl Acad Sci USA. 1999;96(14):7956–61.
Liu C, Wang YQ, Wang YF, Du YY, Song C, Song P, et al. Glycine-serine-rich effector PstGSRE4 in *Puccinia striiformis* f. sp. *tritici* inhibits the activity of copper zinc superoxide dismutase to modulate immunity in wheat. PLoS Pathog. 2022;18(7):1010702.
Livak KJ, Schmittgen TD. Analysis of relative gene expression data using real-time quantitative PCR and the 2(-Delta Delta C(T)) Method. Methods. 2001;25(4):402–8.
Miya A, Albert P, Shinya T, Desaki Y, Ichimura K, Shirasu K, et al. CERK1, a LysM receptor kinase, is essential for chitin elicitor signaling in *Arabidopsis*. Pro Natl Acad Sci USA. 2007;104(49):19613–8.

Nalefski EA, Falke JJ. The C2 domain calcium-binding motif: structural and functional diversity. Protein Sci. 1996;5(12):2375–90.
Oh SK, Young C, Lee M, Oliva R, Bozkurt TO, Cano LM, et al. In planta expression screens of *Phytophthora infestans* RXLR effectors reveal diverse phenotypes, including activation of the *Solanum bulbocastanum* disease resistance protein Rpi-blb2. Plant Cell. 2009;21(9):2928–47.
Panwar V, Jordan M, McCallum B, Bakkeren G. Host-induced silencing of essential genes in *Puccinia triticina* through transgenic expression of RNAi sequences reduces severity of leaf rust infection in wheat. Plant Biotechnol J. 2018;16(5):1013–23.
Pradhan A, Ghosh S, Sahoo D, Jha G. Fungal effectors, the double edge sword of phytopathogens. Curr Genet. 2021;67(1):27–40.
Qi Y, Li JY, Mapuranga J, Zhang N, Chang JY, Shen QH, et al. Wheat leaf rust fungus effector Pt13024 is avirulent to TcLr30. Front Plant Sci. 2023;13:1098549.
Roelfs AP. Race specificity and methods of study. Cereal Rusts Origins Specif Struct Physiol. 1984;1:131–64.
Savary S, Willocquet L, Pethybridge SJ, Esker P, McRoberts N, Nelson A. The global burden of pathogens and pests on major food crops. Nat Ecol Evol. 2019;3(3):430–9.
Schapire AL, Voigt B, Jasik J, Rosado A, Lopez-Cobollo R, Menzel D, et al. *Arabidopsis* Synaptotagmin 1 is required for the maintenance of plasma membrane integrity and cell viability. Plant Cell. 2008;20(12):3374–88.
Segovia V, Bruce M, Shoup Rupp JL, Huang L, Bakkeren G, Trick HN, et al. Two small secreted proteins from *Puccinia triticina* induce reduction of ß-glucoronidase transient expression in wheat isolines containing *Lr9*, *Lr24* and *Lr26*. Can J Plant Pathol. 2016;38(1):91–102.
Shimizu T, Nakano T, Takamizawa D, Desaki Y, Ishii-Minami N, Nishizawa Y, et al. Two LysM receptor molecules, CEBiP and OsCERK1, cooperatively regulate chitin elicitor signaling in rice. Plant J. 2010;64(2):204–14.
Silva KD, Laska B, Brown C, Sederoff HW, Khodakovskaya M. *Arabidopsis thaliana* calcium-dependent lipid-binding protein (AtCLB): a novel repressor of abiotic stress response. J Exp Bot. 2011;62(2679–2689):1460–2431.
Su YY, Chen YE, Chen J, Zhang ZJ, Guo JY, Cai Y, et al. Effectors of *Puccinia striiformis* f. sp. *tritici* suppressing the pathogenic-associated molecular pattern-triggered Immune response were screened by transient expression of wheat protoplasts. Int J Mol Sci. 2021;22(9):4985.
Thomas WJ, Thireault CA, Kimbrel JA, Chang JH. Recombineering and stable integration of the *Pseudomonas syringae* pv. *syringae* 61 hrp/hrc cluster into the genome of the soil bacterium *Pseudomonas fluorescens* Pf0–1. Plant J. 2009;60(5):919–28.
Waheed A, Haxim Y, Islam W, Kahar G, Liu X, Zhang D. Role of pathogen's effectors in understanding host-pathogen interaction. BBA Mol Cell Res. 2022;1869(12):119347.
Wan CP, Liu Y, Tian SX, Guo J, Bai XX, Zhu HC, et al. A serine-rich effector from the stripe rust pathogen targets a Raf-like kinase to suppress host immunity. Plant Physiol. 2022;190(1):762–78.
Wang XY, Li Q, Niu XW, Chen HY, Xu LL, Qi CK. Characterization of a canola C2 domain gene that interacts with PG, an effector of the necrotrophic fungus *Sclerotinia sclerotiorum*. J Exp Bot. 2009;60(9):2613–20.
Wang F, Shen SS, Cui ZC, Yuan ST, Qu P, Jia H, et al. *Puccinia triticina* effector protein Pt_21 interacts with wheat thaumatin-like protein TaTLP1 to inhibit its antifungal activity and suppress wheat apoplast immunity. Crop J. 2023;11(5):1431–40.
Wang BX, Chang JY, Mapuranga J, Zhao CG, Wu YH, Qi Y, et al. Effector Pt9226 from *Puccinia triticina* presents a virulence role in wheat line TcLr15. Microorganisms. 2024;12(8):1723.
Xu Q, Tang CL, Wang XD, Sun ST, Zhao JR, Kang ZS, et al. An effector protein of the wheat stripe rust fungus targets chloroplasts and suppresses chloroplast function. Nat Commun. 2019;10(1):5571.
Xu Q, Tang CL, Wang LK, Zhao CC, Kang ZS, Wang XJ. Haustoria-arsenals during the interaction between wheat and *Puccinia striiformis* f. sp. *tritici*. Mol Plant Pathol. 2020;21(1):83–94.
Yang HJ, Yang SH, Li YQ, Hua J. The *Arabidopsis* BAP1 and BAP2 genes are general inhibitors of programmed cell death. Plant Physiol. 2007;145(1):135–46.
Yang Q, Huai BY, Lu YX, Cai KY, Guo J, Zhu XG, et al. A stripe rust effector Pst18363 targets and stabilises TaNUDX23 that promotes stripe rust disease. New Phytol. 2020;225(2):880–95.
Yin CT, Hulbert SH. Prospects for functional analysis of effectors from cereal rust fungi. Euphytica. 2011;179(1):57–67.
Yin CT, Hulbert SH. Host-induced gene silencing (HIGS) for elucidating *Puccinia* gene function in wheat. Methods Mol Biol. 2018;1848:139–50.
Yin WX, Wang YF, Chen T, Lin Y, Luo CX. Functional evaluation of the signal peptides of secreted proteins. Bio Protoc. 2018;8(9):e2839.
Yokotani N, Ichikawa T, Kondou Y, Maeda S, Iwabuchi M, Mori M, et al. Overexpression of a rice gene encoding a small C2 domain protein OsSMCP1 increases tolerance to abiotic and biotic stresses in transgenic Arabidopsis. Plant Mol Bio. 2009;71(4–5):391–402.
Zhang G, Sun YF, Li YM, Dong YL, Huang XL, Yu YT, et al. Characterization of a wheat C2 domain protein encoding gene regulated by stripe rust and abiotic stresses. Biol Plant. 2013;57(4):701–10.
Zhang L, Shi CC, Li LR, Li M, Meng QF, Yan HF, et al. Race and virulence analysis of *Puccinia triticina* in China in 2014 and 2015. Plant Dis. 2019;104(2):455–64.
Zhang L, Xiao Y, Gao Y, Zhao N, An YJ, Yang WX, et al. Race and virulence analysis of *Puccinia triticina* in China in 2011 and 2013. Plant Dis. 2020a;104(8):2095–101.
Zhang Y, Wei J, Qi Y, Li J, Amin R, Yang W, et al. Predicating the effector proteins secreted by *Puccinia triticina* through transcriptomic analysis and multiple prediction approaches. Front Microbiol. 2020b;11:538032.
Zhang SY, Li C, Si JP, Han ZG, Chen DH. Action mechanisms of effectors in plant-pathogen interaction. Int J Mol Sci. 2022;23(12):6758.
Zhao MX, Wang JF, Ji S, Chen ZJ, Xu JH, Tang CL, et al. Candidate effector Pst_8713 impairs the plant immunity and contributes to virulence of *Puccinia striiformis* f. sp. *tritici*. Front Plant Sci. 2018;9:1294.
Zheng XZ, Wagener N, McLellan H, Boevink PC, Hua CL, Birch PRJ, et al. *Phytophthora infestans* RXLR effector SFI5 requires association with calmodulin for PTI/MTI suppressing activity. New Phytol. 2018;219(4):1433–46.